SOLAR WIND DENSITY MODEL
FROM km-WAVE TYPE III BURSTS

HECTOR ALVAREZ and F. T. HADDOCK

Radio Astronomy Observatory, University of Michigan, Ann Arbor, Mich., U.S.A.

Abstract. The analysis of type III bursts observed from the OGO-5 satellite between 3.5 MHz and 50 kHz (λ 6 km) gives an empirical expression for the frequency drift rate as a function of frequency that is valid from 75 kHz to 550 MHz. Using this expression and some simplifying assumptions we obtain indirectly an empirical formula for the electron density distribution of the solar wind to 1 AU which is consistent with published values of electron density and with observed type III burst drift rates.

1. Introduction

Ground-based observatories have detected type III bursts at frequencies as high as 550 MHz (Maxwell *et al.*, 1960). The lowest frequency at which data has been reported in the literature is of 200 kHz (Slysh, 1967). In a preprint of an unpublished paper N. Dunkel, R. A. Helliwell and J. Vesecky have recently reported the detection of a burst at 25 kHz. This paper presents the results of the analysis of type III bursts observed between 3.5 MHz and 50 kHz by the radiometer that The University of Michigan Radio Astronomy Observatory has aboard the Orbital Geophysical Observatory 5 (OGO-5).

In the high-frequency range type III bursts are characterized by a rapid frequency drift rate (FDR); for example, at 100 MHz it is about 80 MHz s^{-1}; in the low-frequency range the rate is slow, at 100 kHz it is about 10^{-4} MHz s^{-1}. The FDR is a direct consequence of the mechanism of emission of type III bursts: a stream of fast particles originating on the Sun that travels outward through the solar corona producing radio waves at frequencies equal to the fundamental and, in some cases, to the second harmonic of the local plasma frequency. This local plasma hypothesis is assumed in this work. Since the density of the solar plasma decreases with increasing distance from the Sun the type III bursts exhibit a negative FDR. In this paper the negative sign will be implicitly understood. By combining our observations with others we have found a simple empirical expression for the FDR as a function of frequency. The integration * of the FDR empirical expression using some simplifying assumptions to be discussed gave a complicated expression for the coronal electron density as a function of distance. However it could be closely approximated over a wide range of distances by a simple 3-parameters formula. These parameters can be determined by the electron density values at two distances; for example near the Sun and near the Earth, and by the empirical frequency drift rate function. The formula can be applied to the solar wind as well as to solar streamers by adjustment of the parameters.

---

* We thank Dr P. Sturrock for this suggestion made at the AAS Meeting in NYC 1969.

2. The Observations

The radiometer consists of a stepping-frequency receiver and of a monopole antenna. The receiver is of the superheterodyne type with a center frequency tunable in eight steps. The discrete frequencies are 3.5, 1.8 MHz, 900, 600, 350, 200, 100 and 50 kHz. The stepping cycle is completed in 9.2 s and it sets the limit on time resolution of the observations. The 6-db bandwidth of the IF amplifier is 10 kHz.

The antenna unit is a 9.15 m long monopole that protrudes from one of the two solar paddles of the spacecraft. From the other solar paddle, and in the opposite direction, extends a 9.15 m long electrically passive boom. For practical purposes we have considered that the whole structure behaves as a center-fed dipole.

The OGO-5 satellite was launched on March 4, 1968. The initial orbital parameters were approximately the following: height of perigee 292 km, height of apogee 147000 km, inclination to the equator 31°, and period of 63 h 21 min. We notice that height of apogee is about 0.38 of the mean Earth to Moon distance. The radio astronomy antenna was deployed on March 14, 1968.

The data analyzed were obtained between March, 1968 and February, 1970. The data show the presence of spurious signals which can be described as impulsive and nonimpulsive interference. The impulsive interference is seen as sudden increases in the system noise levels followed by equally sudden decreases to the original levels. It is observed simultaneously in different channels. This characteristic provides a mean to discriminate it from the type III solar bursts which show a temporal drift in frequency. The four low-frequency channels were usually affected by this type of unwanted signals. The nonimpulsive interference is seen as a permanent and high noise level in the eight outputs, higher than the preflight receiver noise. This noise level increases with decreasing frequency and it is especially high in the 1.8-MHz and 350-kHz channels.

In connection with the type III solar bursts data we will establish the following definitions: A 'component' is a rise and fall in signal at a given time in a given frequency channel. A 'burst' is a frequency and time sequence of properly related components; a burst may be related to the fundamental or to the second harmonic of the local plasma frequency. An 'event' is a group of bursts generically associated.

We examined 9200 hours of data. Only 79 events were detected in the kilometric wavelength range ($\leqslant 350$ kHz). The number is considerably smaller than the number of hectometric events (~ 2000) largely because of the sensitivity limitation of the four low-frequency channels due to spacecraft interference. For this study we selected only the kilometric wavelength events. Often the receiver was driven to saturation which combined with the discrete character of the telemetry output resulted in loss of time and amplitude resolution.

In this paper we present the results based on 64 of the kilometric wavelength events; the data on 15 were not available at the time of this analysis. The number of events detected at 300, 200, 100 and 50 kHz were 23, 18, 21 and 1, respectively. The 50-kHz event occurred on November 18, 1968 at 1027.7 UT and it was associated with an
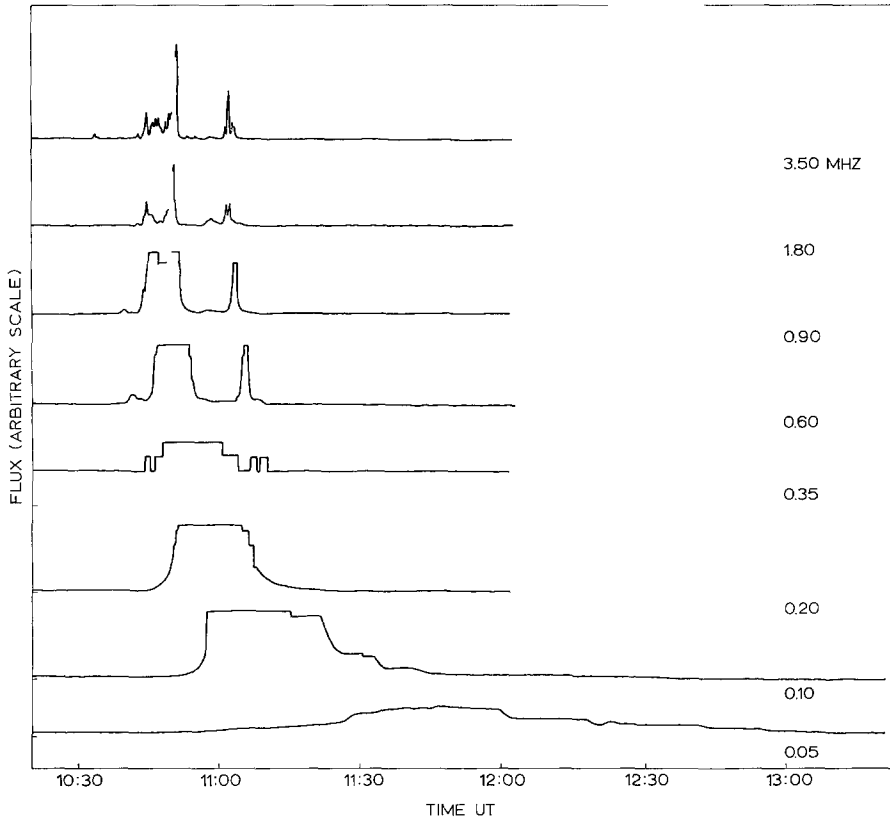
Fig. 1.   Time profiles for the 18 November 1968 event after impulsive interference has been removed. Between 900 and 100 kHz the receiver saturated. The flux density scale at 3.5 MHz is enlarged 10 times.

important solar proton event. The burst profiles of this event are shown in Figure 1. The amplitudes are in a common arbitrary scale, except for the 3.5-MHz scale that is amplified ten times. Marks on the right and on the left indicate zero noise levels. The effects of saturation and of the telemetry quantization can be noted. The radio event began with a group of weak bursts at 1027.7 UT (too weak to be observed in the scale of Figure 1) and continued with a second group of very strong bursts at 1040.0 UT. A study of this radio event was reported earlier by us (Haddock and Alvarez, 1970).

Most of the events studied had a complex time profile. Each event was composed of a succession of bursts that blended in most of the cases. In general the bursts within an event drifted down to different frequencies.

3. Discussion of the Results

3.1. FREQUENCY DRIFT RATES (FDR)

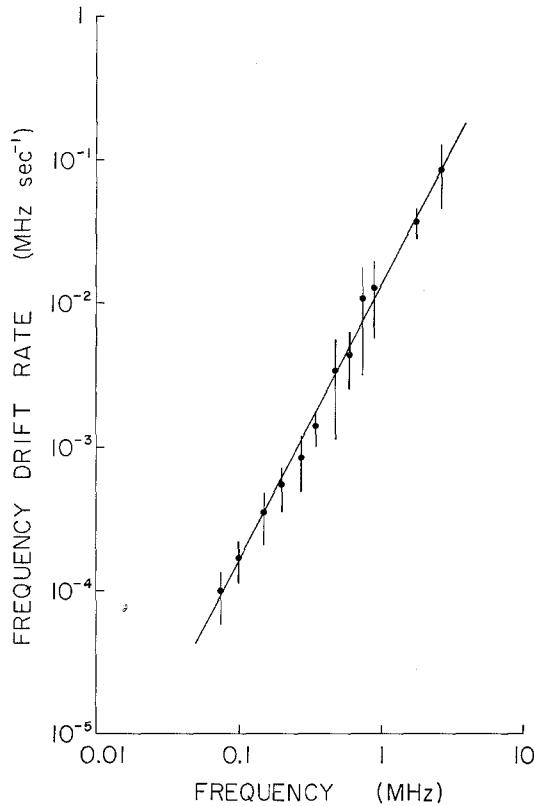The times of start of the components of an event were plotted in graphs displaying

Fig. 2. Frequency drift rates of 18 bursts observed by OGO-5. The straight line represents the least square fit through the averages (dots).

frequency versus time. The first step in the determination of the FDR consisted in drawing, in these plots, a smooth curve through the observed points that presumably belonged to the same burst. The second step was to measure at several frequencies the slope of the curve thus obtained. When possible we drew two extreme curves compatible with the data. This allowed us to estimate the uncertainties in FDR at the selected frequencies. Using this method we measured the FDR of the onset of 52 events.

In a log-log plot the curves of FDR, $|df/dt|$, vs frequency, f, were found to approximate a straight line in 18 events. For the other events available at the time the FDR curves showed abrupt changes in slope; we realized later that this was due to the second harmonic radiation whose existence had been ignored (Haddock and Alvarez, 1971). The measurements of the 18 events are plotted in Figure 2 where the length of the error bars are one standard deviation above and below the average (dots). The general equation of a line through these observations is:

$$\log \left| \frac{df}{dt} \right| = a + \alpha \log f, \tag{1}$$

or:

$$\frac{df}{dt} = -10^a f^\alpha,$$ (2)

where the negative sign has been added in the latter because the starting frequency is observed to drift from high to low values. In our plots we express f in units of MHz and t in seconds. The lease square fit of a straight line through the averages shown in Figure 2 gave for the parameters α and a the values presented in Table I. There σ is the standard deviation of the dispersion of the data points ordinates with respect to the fitted line. We will call α the FDR index.

To investigate the frequency range of validity of this straight-line representation we made a comprehensive search for published information on frequency drift rates. These data are included in Figure 3. They are also observed to fall approximately on a straight line. The parameters of the least-square-fit line are shown in Table I.

TABLE I

Parameters from the least-square-fit of a straight line to the FDR data
$(\log |df/dt| = a + \alpha \log f)$

	α	σ_α	a	σ_a	σ
OGO-5 data (Figure 2)	1.93	0.05	-1.89	0.03	0.08
All data (Figure 3[a])	1.84	0.02	-1.96	0.02	0.19

[a] The data of Young et al. (1961) between 500 and 940 MHz were not used because it is not certain that they correspond to the classical type III bursts (Kundu et al., 1961). However the results of these observers agree with the values expected from an extrapolation of the computed line. They measured FDR larger than 2000 MHz s^{-1}.

The line fitted in Figure 3 to all the observations passes within the error bars of the OGO-5 observations shown in Figure 2, therefore we shall use the parameters derived for the widest frequency range. We conclude that the form of Equation (2) is valid between 550 MHz and 75 kHz and that this equation can be written as:

$$\frac{df}{dt} = -0.01 f^{1.84}, \quad \text{MHz s}^{-1}.$$ (3)

It is remarkable that the data points in Figure 3 fit so well a straight line over seven decades in frequency drift rate, especially when we consider that the observations were made in a variety of circumstances regarding phase of solar cycle, position of associated flares, velocities of bursts exciters, electron density distribution of the solar corona, etc.

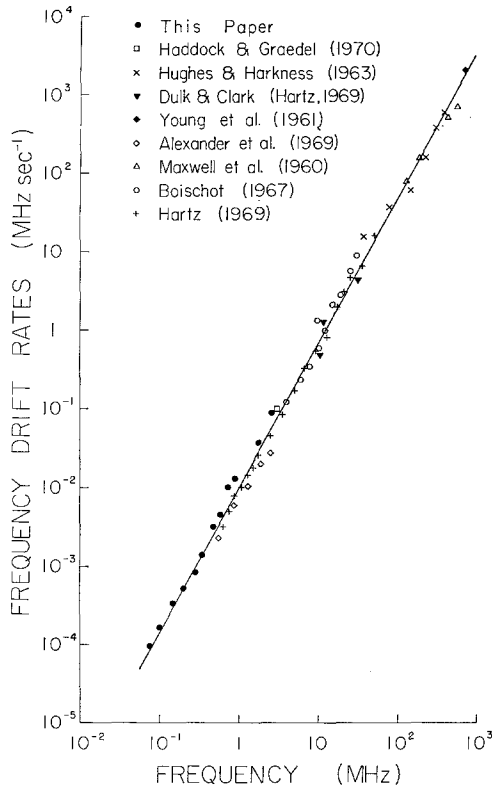Wild (1950) wrote an analytical expression for the FDR as a function of frequency

Fig. 3. Observed frequency drift rate of type III bursts. The straight line represents the least square fit. The observations cover one complete 11-yr cycle.

of the same form as Equation (2) but he used $\alpha = 1$. We will see in discussing Equation (6) that this value is ruled out in our models.

The importance of Equation (3) lies in the fact that, as far as we know, it is the only empirical relationship available in the region extending out to a large fraction of an AU, and furthermore it provides a new approach to study the electron density of the solar corona in a range of distances rather inaccessible at present.

3.2. THE ELECTRON DENSITY DISTRIBUTION OF THE SOLAR CORONA

By making some simplifying assumptions Equation (3) leads to a simple differential equation involving the coronal electron density, the distance from the Sun and other parameters. The assumptions are the following: (a) For the emission mechanism we assumed the local plasma hypothesis. (b) For the shape of the trajectory of the exciter particles we choose an Archimedes spiral as suggested by solar wind studies. For simplicity we assumed that the trajectories are contained in the plane of the ecliptic. The velocity of the solar wind was also assumed to be constant and equal to 260 km s^{-1}; this means that exciter particles originating on the west limb will pass through the Earth. (c) We assumed that the exciter particles travelled with constant velocity and

zero pitch angle along a spiral. We will express velocities in terms of fractions, β, of the velocity of light in vacuum, c. (d) In a nonhomogeneous plasma a ray undergoes refraction and scattering effects. These effects were ignored and for simplicity we have assumed that the electromagnetic waves travel from the burst source to the Earth as in a vacuum.

The electron density gradient can be written as:

$$\frac{dN}{dr} = \frac{dN}{df} \frac{df}{dt} \left(\frac{ds}{dt}\right)^{-1} \frac{ds}{dr}, \tag{4}$$

where N is electron density, f is frequency, t is time, s is path length along the spiral and r is radial heliocentric distance. The different derivatives can be obtained as follows: dN/df, from the plasma frequency equation; df/dt, from the empirical formula (3); ds/dr, from the Archimedes' spiral equation, and ds/dt, is the exciter velocity.

The definite integration of Equation (4) between r_0 and r gives (Alvarez and Haddock, 1970):

$$N = \frac{D}{\left[\left\{\frac{D}{N(r_0)}\right\}^{(\alpha-1)/2} + \frac{1}{\beta}\left\{s(r, \varepsilon) - s(r_0, \varepsilon)\right\} + x(r, \varepsilon, \theta_F) - x(r_0, \varepsilon, \theta_F)\right]^{2/(\alpha-1)}}, \tag{5}$$

where:

$$D = \left\{\frac{c\,10^{-a}}{(\alpha-1)(9j)^{\alpha-1}}\right\}^{2/(\alpha-1)}$$

and j equals 1 and 2, for fundamental and second harmonic of the plasma frequency, respectively; r_0 is an arbitrary radial distance at which the electron density is assumed to be known and x is the distance between the burst source and the Earth. Both s and x depend on the parameter ε that determines the tightness of the spiral (in this study we adopted arbitrarily $\varepsilon = \pi/2$); x depends also on θ_F, the orientation of the spiral as measured from the Sun's central meridian. The other parameters have been defined. Curves 1 and 2 of Figure 4 show electron density distributions from Equation (5) for two values of θ_F with the other parameters unchanged. It was assumed that Equation (3) is valid out to 1 AU, and the electron density was fixed at $r_0 = 1$. The parameters a and α, not included in Table I, were adopted from a preliminary determination and are used here only for comparison.

Strictly speaking we should apply Equation (5) to each of the bursts studied and obtain an electron distribution $N(r)$ from each of them. Some of the parameters should be known (α, a, and θ_F), others could be estimated within reasonable limits (ε and $N(1)$) and others (j and β) could be determined by requiring that the curve pass through the electron density value measured near the Earth. We did not do this because of problems in interpretation of the FDR curves of some bursts. These problems were solved later (Haddock and Alvarez, 1971). What we did was to look for an analytical function which closely approximates Equation (5) over a wide range of distances, that would be simple and still compatible with the observations of electron
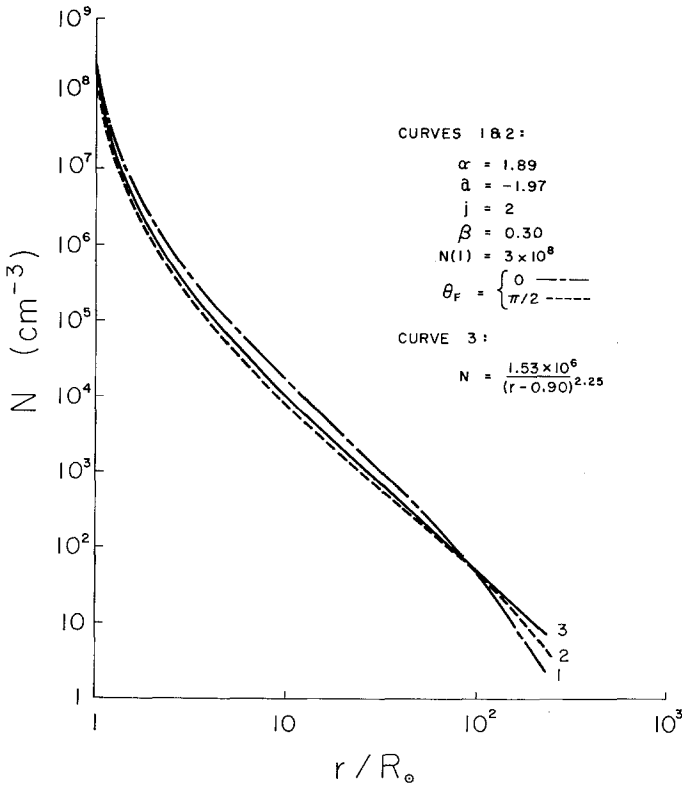
Fig. 4.   Comparison of two electron density models for some typical parameter values. Curve 3 from Equation (6), resembles curves 1 and 2, from Equation (4), within the range of validity of the empirical frequency drift rate formula.

density and of the FDR of type III bursts. We obtained the following expression (Alvarez and Haddock, 1971):

$$N(r) = \frac{A}{(r-b)^p},$$ (6)

where

$$p = \frac{2}{\alpha - 1}.$$ (7)

Curve 3 of Figure 4 shows this function with the parameters for $N(1) = 3 \times 10^8$ cm^{-3}, $N(100) = 10$ cm^{-3} and $p = 2.25$, corresponding to $\alpha = 1.89$.

Most of the bursts analyzed were associated with flares on the western hemisphere of the Sun, for this reason we choose for comparison in Figure 4 center disc $(\theta_F = 0)$ and west limb $(\theta_F = \pi/2)$ associated flares. Beyond about 150 $R_\odot$ curves 1 and 2 exhibit a dropping off due to the proximity of the burst source to the Earth; this is a direct consequence of assuming that the FDR Equation (3) is valid out to 1 AU.

We will attempt to show that formula (6) gives values of electron density and frequency drift rates in agreement with observations over a wide range of distances, almost 1 AU.

It is desirable to determine the parameters A, b and p in such a way that the resulting numerical model is consistent with observed electron densities and frequency drift rates. In an attempt to fulfill this last condition we chose tentatively $\alpha = 1.84$ from Table I; this gives $p = 2.38$. The parameter A is best determined by the electron density observed near the Earth, $N(215)$. Within the wide range of values of N measured near the Earth (Montgomery et al., 1968; Neugebauer and Snyder, 1966; etc.) we choose arbitrarily the three values 31, 7.7 and 4.0 cm^{-3}, corresponding to plasma frequencies of 50, 25 and 18 kHz, respectively. Parameter b is best determined by the electron density near the Sun, $N(1)$. Because type III bursts have been observed at frequencies as high as 550 MHz the electron density near the Sun can not be smaller than 3.73×10^9 cm^{-3}, at least when these bursts were observed. The distance of the plasma level at 550 MHz is not known precisely, and it varies with time and position. The exact value is not important in this study. For simplicity we took it at $1\ R_\odot$.

In order to test the practicality of formula (6) we adopted three models whose parameters are given in Table II.

TABLE II

Characteristics of some electron density models of the solar corona
$(N(r) = A(r - b)^{-2.38})$

Model	$N(1)$ (cm^{-3})	$N(215)$ (cm^{-3})	$b\,(R_\odot)$	A (cm^{-3})
I	4.4×10^8	4.0	0.91	1.41×10^6
II	4.0×10^9	7.7	0.95	2.75×10^6
III	4.0×10^9	31	0.91	1.12×10^7

Models I and II correspond to typical solar wind densities. At the base the coronal Model I is not sufficiently dense to give a plasma frequency of 550 MHz. This is not the case in Model II and III. Model III is about four times denser than Model II away from the Sun. Plots of these models are shown in Figure 5. This figure includes optically determined values of $N(r)$ near the Sun and direct measurements of it from artificial satellites near the Earth. By construction the models fit the observations near the Sun and near the Earth. Models I and II show a good fit to observations at intermediate distances $(5-20\ R_\odot)$, and therefore presumably good estimates of $N(r)$ between $20-215\ R_\odot$.

For distances beyond the Earth's orbit where there are no direct measurements of $N(r)$ Equation (6) closely approximates most theoretical solar wind models. In fact, in a $\log N$ vs $\log r$ plot many theoretical models approximate a straight line for large r; the slope of this line is p. Using this approximation when feasible we measured p in the range between 2.09 (Cuperman and Harten, 1971, Figure 2) and 2.28 (Whang et al.,
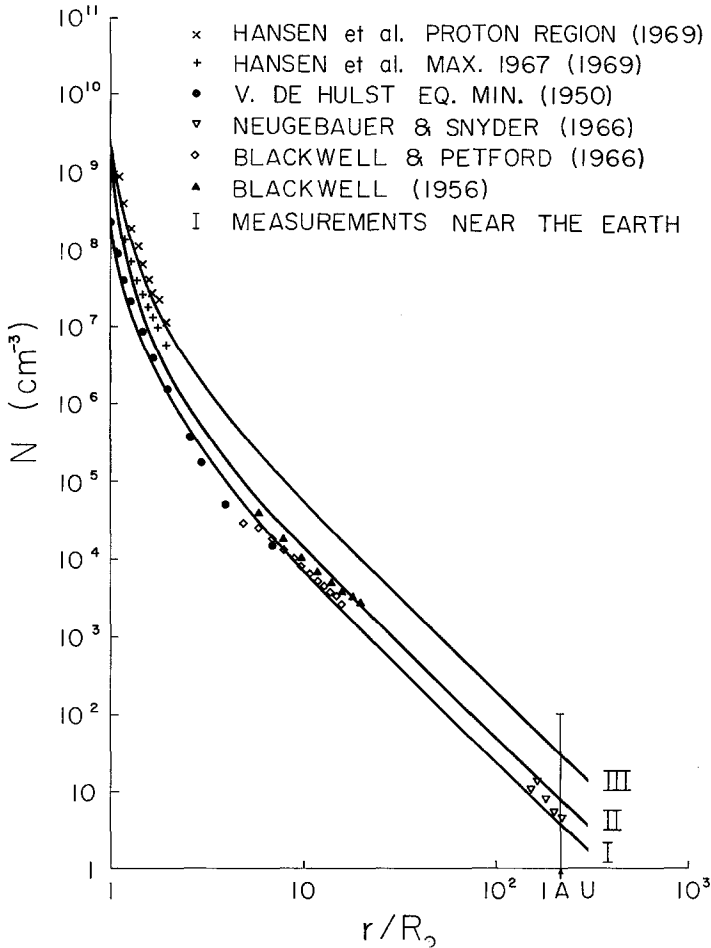
Fig. 5.   Comparison of electron density models based on Equation (6) with optical
and particle observations.

1966). Observations within 1 AU give values between 2.3 (Blackwell and Petford, 1966) and ∼3 (Neugebauer and Snyder, 1966).

As a final check we derived the expression for the frequency drift rate using Equation (6) and the assumptions discussed earlier and then compared it with the observations of FDR for type III bursts. The resulting expression is of the form:

$$\log \left| \frac{df}{dt} \right| = a + \alpha \log f - \Delta, \tag{8}$$

where a is a function of p, A, β, j, as defined earlier. α is given by Equation (7). Δ depends on f, ε and θ_F and it is a slowly varying function of frequency, except when the trajectory of the exciter particles passes through or very near to the Earth. Except
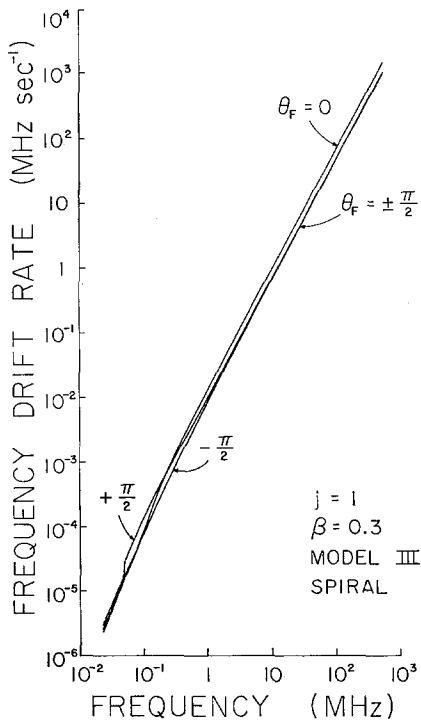
Fig. 6. Frequency drift rate curves derived from Equation (6) for different orientations of the spiral trajectory.

for the term A, Equation (8) is of the same form as Equation (1). To plot Equation (8), we used $p=2.38$ and considered β, θ_F, j, ε and A as parameters. Some of the results are shown in Figure 6. The curves $\log|df/dt|$ vs $\log f$ are fairly straight above 0.5 MHz. Below this frequency the curves drop with decreasing frequency with respect to the straight line defined at higher frequencies. This may indicate the reality of the fact that the FDR index of the OGO-5 data is somewhat larger than that of all data (see Table I). In Figure 6 we observe that bursts originating in the west or east limb give not too different drift rate curves. These curves are separated in $\log|df/dt|$ approximately by σ, the dispersion of the observed points from the fitted line in Figure 3 (see also Table I). The curves computed for $j=1$ (fundamental) and $j=2$ (second harmonic), not shown, are similar and also seperated by approximately σ. We conclude that the simple formula of Equation (6) is consistent with the observed frequency drift rates.

The range of accuracy of Equation (6) in representing electron density models, and especially its simplicity should be useful for calculations that involve refraction or/and scattering of radio waves (from solar or extrasolar sources) by the corona, or dispersive effects on pulsar signals, etc. Equation (6) is a simpler variant of the Baumbach type of empirical formula (Baumbach, 1937).

Formula (6) also fits the density distribution in solar streamers and can thus be

used in place of the inverse power series generally adopted by various authors. The parameters A, b, and p can be determined from a three-point fit. For example, the the observations of Newkirk et al. (1970) of the southwest streamer can be represented to within 10% by formula (6) with $A = 7.41 \times 10^6$ cm^{-3}, $b = 0.60\, R_\odot$, and $p = 2.86$.

4. Conclusions

The OGO-5 radio astronomy instrument has extended the detection of type III solar bursts down to 50 kHz.

The observed frequency drift rate is a simple power function of the frequency, in the range between 550 MHz and 75 kHz. This function leads to an approximate formula for the electron density distribution models of the solar wind. An appropriate choice of the parameters makes this three parameter formula consistent with the observations of electron density and frequency drift rate. The formula has been shown to be good approximation to $N(r)$ between 1 $R_\odot$ and 1 AU thereby filling the gap in observational data on $N(r)$ in the region 20–200 $R_\odot$. It should also be useful to compute refraction, scattering and dispersion of radio waves by the corona. Beyond 1 AU our model is not inconsistent with theoretical models. The formula can be fit to solar streamers.

Acknowledgements

Note added in proof. The paper by N. Dunkel, R. A. Helliwell, and J. Vesecky was published in *Solar Phys.* **25** (1972), 197.

Also J. Fainberg, L. G. Evans, and R. G. Stone have recently reported the detection of bursts at 30 kHz. (*Science* **178** (1972), 743.)

References

Alexander, J. K., Malitson, H. H., and Stone, R. G.: 1969, *Solar Phys.* **8**, 388.
Alvarez, H. and Haddock, F. T.: 1970, *Bull. Am. Astron. Soc.* **2**, No. 4, 291.
Alvarez, H. and Haddock, F. T.: 1971, URSI Meeting, Washington, D.C., April.
Baumbach, S.: 1937, *Astron. Nachr.* **263**, 121.
Blackwell, D. E.: 1956, *Monthly Notices Roy. Astron. Soc.* **116**, 56.
Blackwell, D. E. and Petford, A. D.: 1966, *Monthly Notices Roy. Astron. Soc.* **131**, 399.
Boischot, A.: 1967, *Ann. Astrophys.* **30**, No. 1, 85.
Cuperman, S. and Harten, A.: 1971, *Astrophys. J.* **163**, 383.
Dulk, G. A. and Clark, T. A.: 1969, *Planetary Space Sci.* **17**, 267.
Haddock, F. T. and Graedel, T. E.: 1970, *Astrophys. J.* **160**, 293.
Haddock, F. T. and Alvarez, H.: 1970, *Bull. Am. Astron. Soc.* **2**, No. 2, 196.
Haddock, F. T. and Alvarez, H.: 1971, *Bull. Am. Astron. Soc.* **3**, No. 1, Part 1, 6.
Hansen, R. T., Garcia, C. J., Hansen, S. F., and Loomis, H. G.: 1969, *Solar Phys.* **7**, 417.
Hartz, T. R.: 1969, *Planetary Space Sci.* **17**, 267.
Hughes, M. P. and Harkness, R. L.: 1963, *Astrophys. J.* **138**, 239.

Kundu, M. R., Roberts, J. A., Spencer, C. L., and Kuiper, J. W.: 1961, *Astrophys. J.* **133**, 255.

Maxwell, A., Howard III, W. E., and Garmire, G.: 1960, *J. Geophys. Res.* **65**, 3581.

Montgomery, M. D., Bame, S. J., and Hundhausen, A. J.: 1968, *Trans. Am. Geophys. Union 49th Annual Meeting*, p. 262.

Neugebauer, M. and Snyder, C. W.: 1966, *J. Geophys. Res.* **71**, 4469.

Newkirk, G., Jr., Dupree, R. G., and Schmahl, E. J.: 1970, *Solar Phys.* **15**, 15.

Slysh, V. I.: 1967, *Cosmic Res.* **5**, 759 (1967, *Kosm. Issled.* **5**, 897).

Van de Hulst, H. C.: 1950, *Bull. Astron. Inst. Neth.* **11**, 135.

Whang, Y. C., Liu, C. K., and Chang, C. C.: 1966, *Astrophys. J.* **145**, 255.

Wild, J. P.: 1950, *Australian J. Sci. Res.* **A3**, 541.

Young, C. W., Spencer, C. L., Moreton, G. E., and Roberts, J. A.: 1961 ,*Astrophys. J.* **133** .243.